Contrib Mineral Petrol (1990) 104:73–84

Contributions to Mineralogy and Petrology

The record of magma chamber processes in plagioclase phenocrysts at Thera Volcano, Aegean Volcanic Arc, Greece

Karen Stamatelopoulou-Seymour[1], Dimitrios Vlassopoulos[2], Thomas H. Pearce[3], and Craig Rice[3]

[1] Department of Geology, Concordia University, Montréal, Québec, H4B 1R6, Canada
[2] Department of Geological Sciences, McGill University, Montréal, Québec, H3A 2A7, Canada
[3] Department of Gological Sciences, Queen's University, Kingston, Ontario, K7L 3N6, Canada

Abstract. Lavas and pyroclastic rocks throughout the volcanic stratigraphy of the Tertiary-Quaternary volcanic complex of Thera in the Aegean island arc display inhomogenous plagioclase populations and phenocryst resorption textures, interpreted as indicative of magma mixing. Plagioclase zoning characteristics studied by Nomarski and laser interferometry techniques establish three main categories of plagioclase: (i) inherited plagioclase (nucleated in end-member prior to initial mixing event) (ii) in situ plagioclase (nucleated in mixed or hybrid magma) and (iii) xenocrystic plagioclase. Nomarski contrast images and linearized compositional zoning profiles reveal striking differences between calcic and sodic plagioclases, depending on the composition of the lava in which they are hosted. These differences reflect the contrasting effects of changes in physical-chemical parameters in basic vis-a-vis more acidic melts during magma mixing and/or influx of new magma into the subvolcanic magma chamber, as well as the influence of magma chamber dynamics on plagioclase equilibration. Variations in bulk major and trace element abundances of Thera volcanic products reflect the dominant overprint of crystal fractionation, but decoupling between major and trace element fractionation models and variations in incompatible trace element distributions are all indicative of magma mixing processes, consistent with compositional and textural zoning in plagioclases.

Introduction

Disequilibrium phenocryst populations are typical of andesites, and provide sensitive indicators of magma mixing (MacDonald and Katsura 1965). Plagioclase is particularly revealing because it is the most abundant and ubiquitous phenocryst mineral in orogenic suites (Gill 1981) and has a good memory due to sluggish NaSi – CaAl diffusion rates. Zoned plagioclases from the volcanic complex of Thera (Figs. 1 and 2) were investigated for variations with stratigraphic position and host composition (basalt-dacite). Laser, Nomarski interferometry and electron microprobe techniques were employed.

Offprint requests to: K. Stamatelopoulou-Seymour

Volcanology of Thera

The active volcanic complex of Thera is the most studied in the Aegean Volcanic Arc. Volcanic activity dates back to at least 1.0 Ma (Seward et al. 1980). During the catastrophic Minoan eruption of ca 1400 B.C. (Hammer et al. 1987), the extensive Minoan Tuff (Upper Pumice Series or Ober Bimstein) was deposited, and was followed by caldera collapse of the precaldera island of Strongyle (Greek for "round"). The pre-Minoan Thera volcanoes developed from vents along a NE-trending graben which apparently still controls the location of post-caldera volcanic activity (Kameni islands, Fig. 2). The complex was built up in the northern part from three overlapping subaerial lava shield volcanoes (Skaros, Therasia, and Megalo Vouno, Fig. 2), while the southern part was occupied by a submerged vent (Akrotiri) which produced phreato-

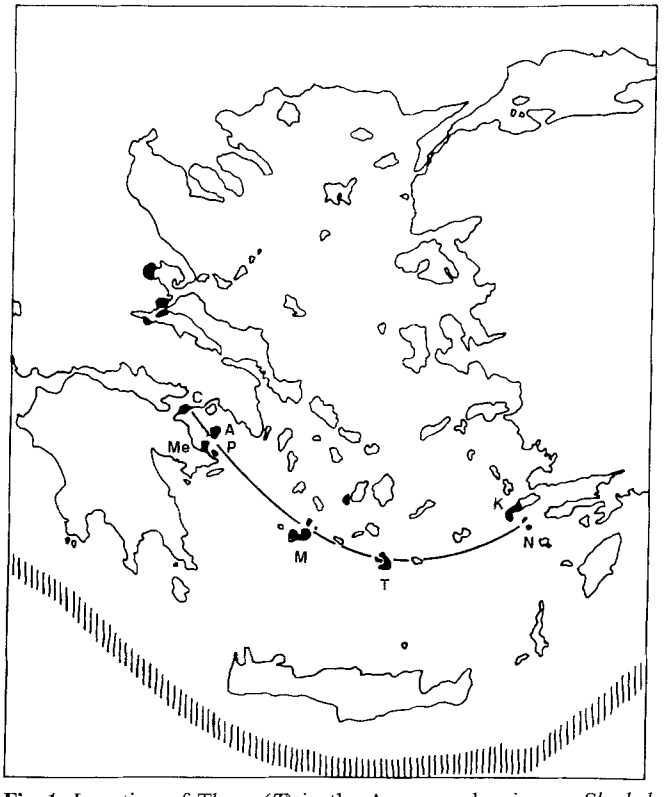

Fig. 1. Location of Thera (*T*) in the Aegean volcanic arc. *Shaded strip* indicates position of trench

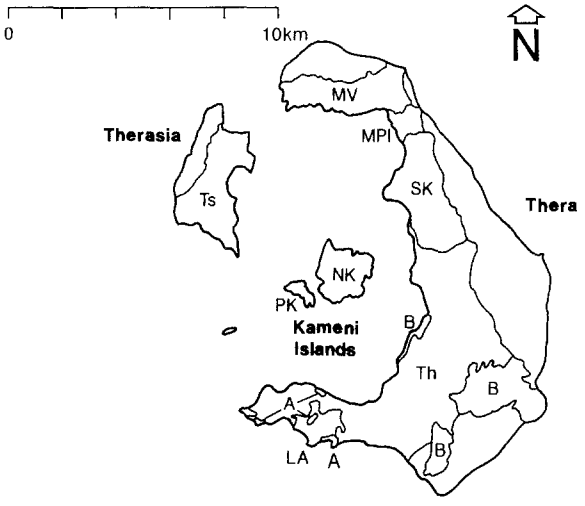

Samples studied

MODERN SERIES	NK	Nea Kameni +	dacite: NK-1,-7,-10,-12
	PK	Palea Kameni	
		Bo caldera	
MAIN SERIES	SK	Skaros □	basalt: MP-1
	Ts	Therasia	
	MPI	Mikros Profitis Ilias ■	andesite: MP-2,-2B
		Bu caldera	
	MV	Megalo Vouno ▲	basalt: OIA-2 andesite: OIA-1
	Th	Thera △	basalt: T-2 dacite: T-1
	A	Akrotiri ●	basalt: A-1 andesite: A-2 dacite: A-3,-5,-7
	LA	Lumaravi-Archangelo	
Basement	B	limestone, schist	

Fig. 2. Geological sketch map of Thera and volcano-stratigraphic column with stratigraphic locations and descriptions of samples used in this study

magmatic tuff deposits (Middle Tuff Sequence, Heiken and McCoy 1984). These tuffs were erupted along the walls of an older caldera formed 0.1 Ma ago (Seward et al.1980) during the eruption of the Lower Pumice Series (Unter Bimstein). At present, volcanic activity persists at Nea Kameni island, in the center of the inundated Minoan caldera (Fig. 2). The hyalodacitic domes and flows of the Kameni islands are reported not to have undergone significant chemical evolution during the last 2200 years (Barton and Huijsmans 1986). The most recent eruption on Nea Kameni occurred in 1954. A synopsis of the volcanic stratigraphy of the Thera volcanic complex is presented in Fig. 2. Volcanic products range in composition from basalt to rhyodacite, and occur as flows and predominantly pyroclastic deposits with the Minoan Tuff representing a volume of 3 to 18 km^3 of ejecta (Watkins et al. 1981).

Methods

Two thin sections were cut from samples of five different lava flows. About twelve "optimum" crystals from the over 800 plagioclase phenocrysts per slide were chosen for study by laser and Nomarski contrast interferometry. Selection criteria were: (1) that the crystal be sectioned through its core and (2) have zones perpendicular to the plane of the section. For further discussion, see Pearce (1984).

Nomarski contrast interferometry

Nomarski interference contrast imaging reveals spectacularly enhanced zonal and discontinuous features in etched plagioclase phenocrysts (Anderson 1983; Clark et al. 1986). Etching a polished thin section with concentrated HBF_4 preferentially etches the more calcic zones in plagioclase crystals. The result is a microtopographic relief of highs (more sodic, less calcic) and lows (less sodic, more calcic), in which the compositional variations in the crystals are visually enhanced. Etched thin sections are carbon-coated to increase reflectivity and eliminate internal reflections. Nomarski imaging reveals very fine textural details not visible in transmitted light, but does not readily indicate absolute compositions (Fig. 3).

Laser interferometry

Laser interference microscopy is ideal for direct observation and analysis of compositional changes in zoned minerals. An interferogram of a crystal shows changes in refractive index (due to changes in composition) across the crystal as shifts in narrow interference fringes. A complete description of the technique is given by Pearce (1984).

Using coherent green light ($\lambda = 514.5$ nm) produced by a Spectra-Physics 164 Argon-ion laser, the source beam passes through a spatial filter and collimator. This expands the beam and produces a planar wavefront. A beam-splitter then separates the light into reference and sample beams. The sample beam is diverted to travel through a plagioclase crystal in a polished thin section. In so doing, it becomes encoded with information of the magnitude and distribution of refractive index in the crystal. Interference of this beam with the reference beam results in narrow, parallel light and dark fringes with displacements that are directly related to changes in refractive index and, hence, compostion.

The interferograms in Figs. 4c, 5c, 6c, and 7c may be interpreted as graphs of plagioclase composition. They are customarily oriented with An content increasing towards the top of the photo. A fringe displacement of one wavelength (normal distance across one one light and dark fringe pair) corresponds to a change of composition of 33 mole % An. Photographic recording and subsequent digitization of fringe profiles establishes accurate relative compositional profiles across plagioclase crystals. Microprobe analysis of selected points in the crystals enables the calibration of these profiles in terms of absolute An composition.

Electron microprobe

Plagioclase, olivine and pyroxene compositions were determined with the Cameba Camebax electron microprobe unit at McGill

Fig. 3A–H. Nomarski images from etched surfaces of plagioclase crystals illustrating various growth and solution features. **A** Crystal A-5-10 from Akrotiri dacite. The interior of this crystal is strongly "mottled" obscuring the original zonation. Subsequent growth on this mottled core resulted in convolute zoning which tends to more euhedral zones in the outer parts of the crystal (*C*). **B** Crystal T-2-3 from Thera basalt. This crystal exhibits very little zoning other than two resorption surfaces (*R*). These surfaces are rough and jagged in nature, suggestive of relatively large volume loss during the solution events. **C** Microphenocryst MP-1-5 from Skaros basalt. This euhedral crystal is in the groundmass of the sample. Growth was so consistent in this crystal that the zones form a line where they meet at corners. Careful examination shows that the core of this crystal is discordant with later zones suggesting a change of conditions early in growth (*D*). **D** Phenocryst MP-1-4 from the same sample. This crystal morphology is common in this sample. The core of the phenocryst is mottled (*M*). Growth beyond the core appears similar to that seen in **A** above. **E** Phenocryst MP-2-2 from Mikros Profitis Ilias andesite. The interior zones of this crystal are prominently cross-cut by zones following a major resorption period (*R*). Continued growth resulted in the inclusion of groundmass material (*I*) and the entrainment of an opaque mineral (*O*). **F** Phenocryst MP-2-3 from the same sample. Consistent with the crystal above, considerable volume loss is indicated by resorption surface in this crystal (*R*). Large embayments and smooth round surfaces characterize this solution event. Subsequent growth infilled

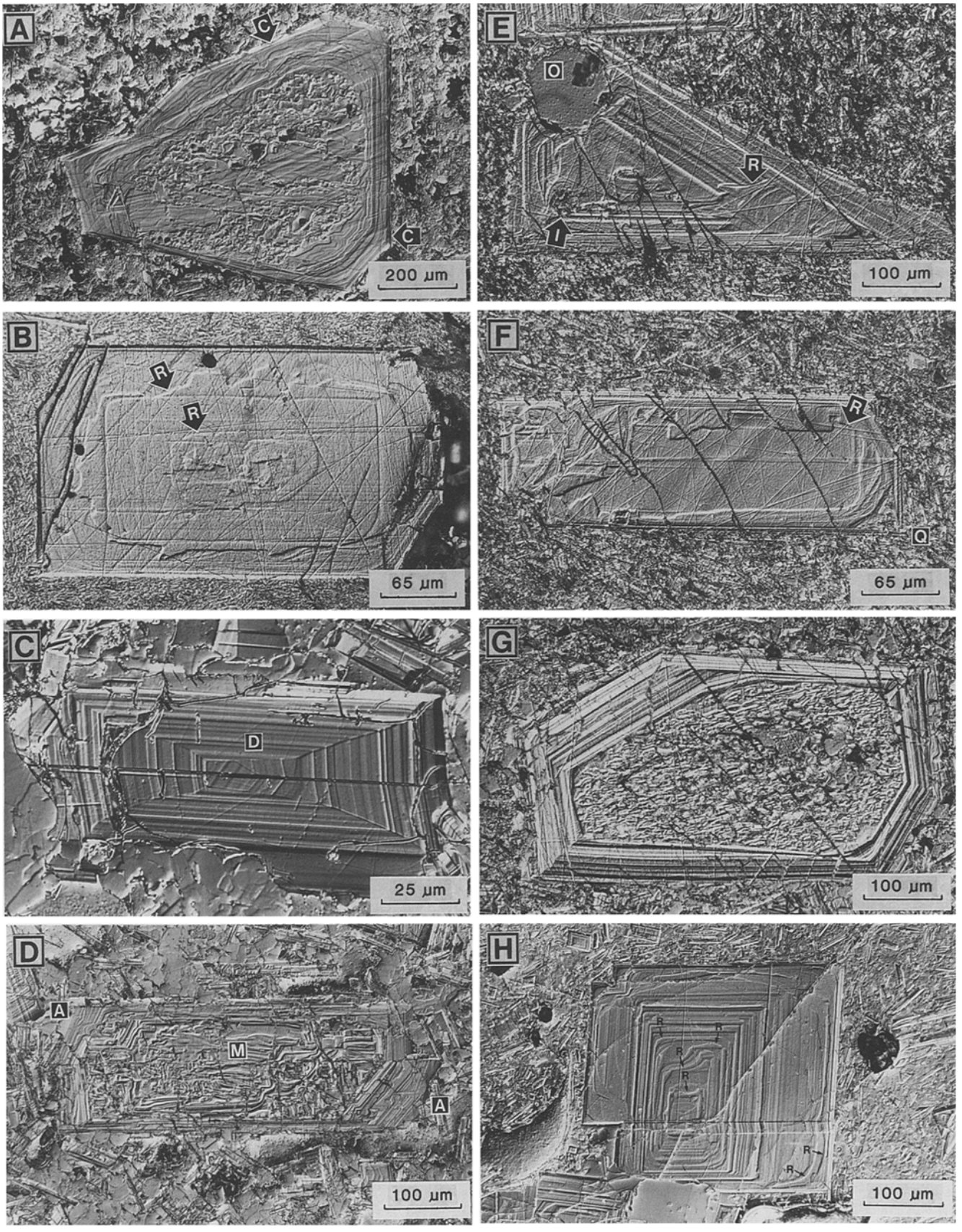

the embayments and ended with a quench style of growth at one corner (*Q*). **G** Phenocryst OIA-2-3 from Megalo Vouno basalt. Similar to crystal T-2-4 of this crystal shows a fritted, inclusion-rich core that is rounded. Resumed growth resulted in a euhedral shape with no further evidence of solution. **H** Phenocryst NK-7-9 from Nea Kameni dacite. This crystal shows numerous minor resorption surfaces (*R*) yet it has maintained a more or less euhedral shape throughout its growth history.

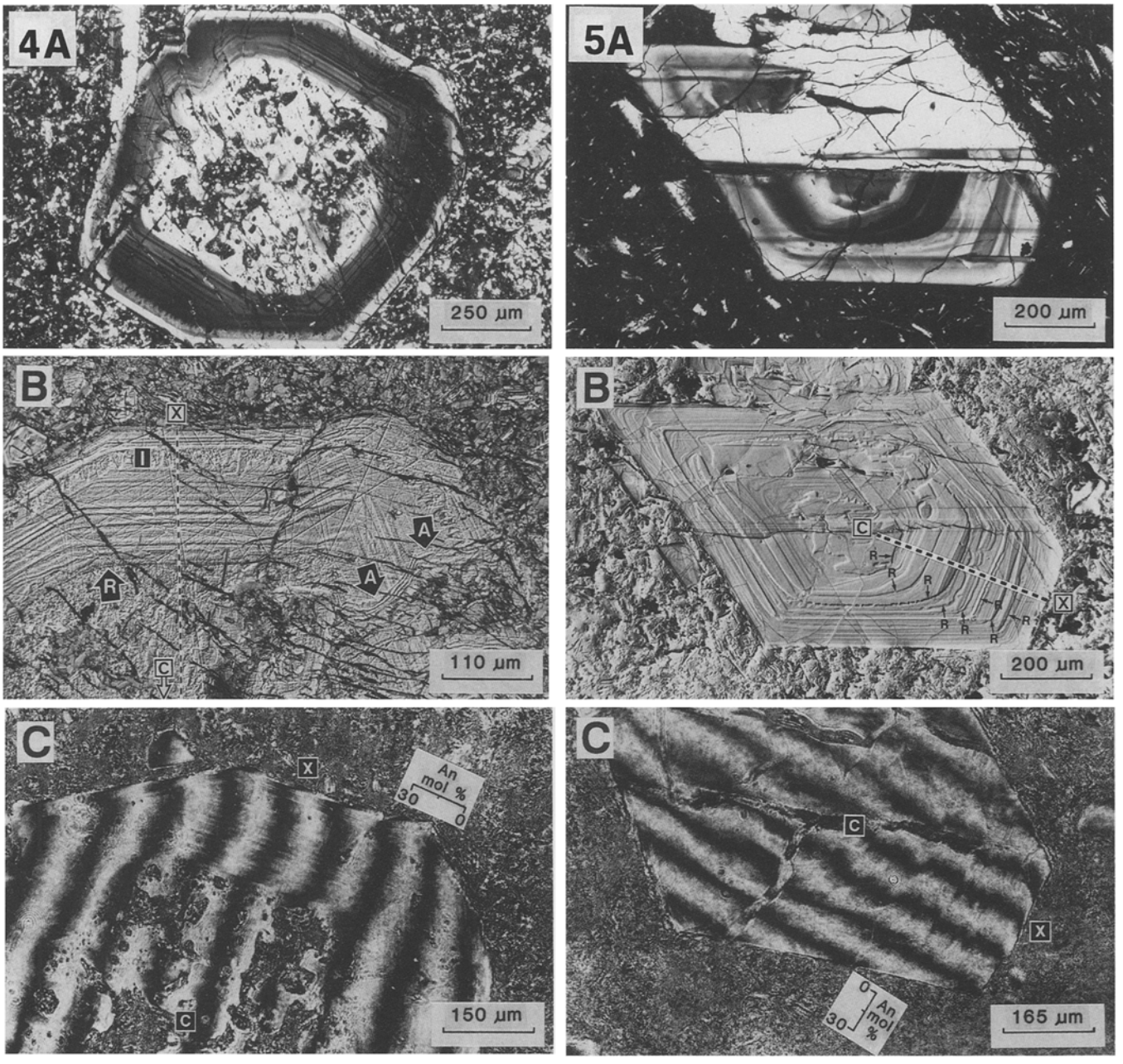

Figs. 4–7. Cross-polarized (**A**), Nomarski contrast images (**B**), and narrow fringe laser interferograms (**C**) of examples of the main types of plagioclase recognized in Thera lavas

Fig. 4A–C. Type Ia inherited plagioclase, OIA-2-1. **A** Spongy core followed by more sodic mantle and calcic rim. **B** The Nomarski image is a close-up of the right side of the photomicrograph. The core is separated from the mantle by a resorption surface (*R*). A zone of inclusions (*I*) defined by a sawtooth resorption surface precedes the calcic rim. The remnant of a channel through the mantle to the core is also noted **A**. **C** C–X marks the fringe used to construct the profile in Fig. 13a. The fringe trace is essentially flat through the core, with various oscillations in the mantle, and a jump at the rim. An scale is relative

Fig. 5A–C. Type Ib inherited plagioclase, A-5-3. **A** Oscillatory zoning is evident as well as smooth rounded resorption surfaces. **B** Prominent resorption surfaces (*R*) are emphasized in the Nomarski image as well as some not recognized in **A**. **C** *C–X* indicates the fringe used to construct Fig. 13b

Fig. 6A–C. Type II in situ-plagioclase, NK-7-13. **A** Oscillatory zoning and a resorption surface (*R*) with an embayment marked by an inclusion (*I*) are evident. **B** A number of resorption surfaces are revealed in the Nomarski image. The shape of the embayment suggests that significant crystal volume was lost during the resorption event. **C** *C–X* marks the fringe used to construct Fig. 13c. The fringe trace is essentially flat in the in the core and more oscillatory outwards

Fig. 7A–C. Type III xenocrystic plagioclase, T-2-4. **A** This crystal has a fritted core and is normally zoned. **B** A resorption surface (*R*) bounds the core. Continued growth is evidenced by numerous euhedral zones. **C** *X–Y* indicates fringe used to construct Fig. 13d.

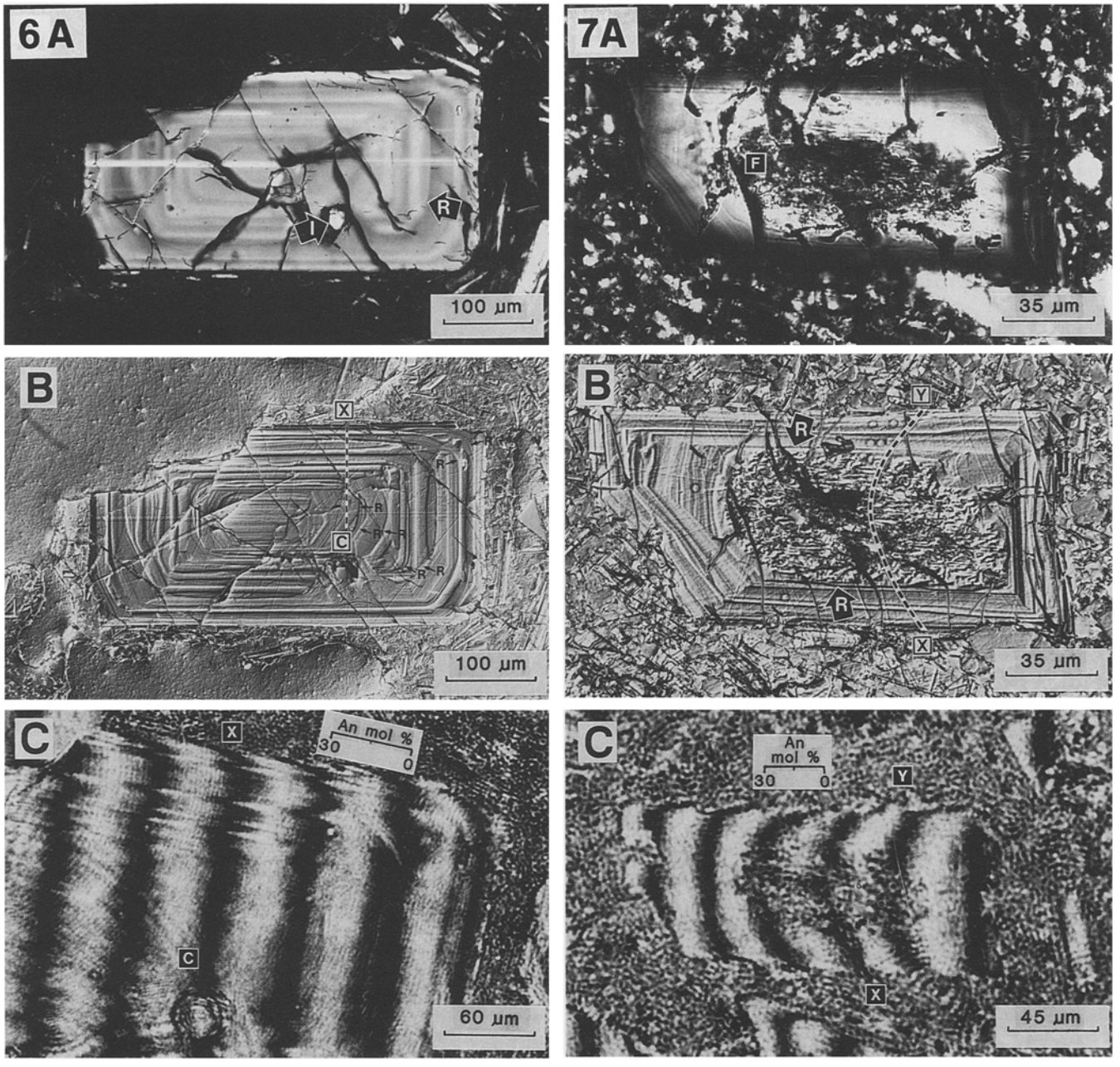

The fringe trace has a prominent curvature and the core has a composition of An_{90}. The fritted core is suggestive of decompression, as discussed in the text

University (15 kV accelerating potential, 80 nA electron beam current, 10 µm beam, width, counting time 25 seconds). Selected points along plagioclase profiles were analysed in order to calibrate the laser interferometry profiles, and traverses across selected olivine and pyroxene crystals with spacing between analyses ranging from 10 to 50 µm were performed.

Petrochemistry

The magmas extruded as lavas or pyroclastics from individual centers on Thera range in composition from andesitic basalt to rhyodacite (Nicholls 1971; Huijsmans et al. 1988), with the exception of the Recent Series whose compositions are restricted to dacite (Barton and Huijsmans 1986). Variations in bulk chemistry based on our own unpublished major and trace element data as well as data published by these authors clearly show the predominant role of fractionation of the observed phenocrystic assemblages in the geochemical evolution of the Thera volcanics. Although major and compatible trace element variations are rather insensitive to magma mixing processes, incompatible trace elements are better indicators of processes involving more than one end-member. Plots of one incompatible trace element abundance ratio against another (Fig. 8) suggest parabolic trends which are characteristic of linear mixing between two end-members (Langmuir et al. 1977). Furthermore, Zr-normalized Y-Rb systematics (Fig. 9) indicate a strong contribution from a continental crustal component (assimilation) to the early Akrotiri center magmas (A), whereas the younger Main Series lavas (M) show a continuous and extensive range of Rb/Y, evidence of inputs from at least two sources to the magma budget. On the other hand, the post-caldera lavas of Kameni (K) cluster in a relatively restricted field.

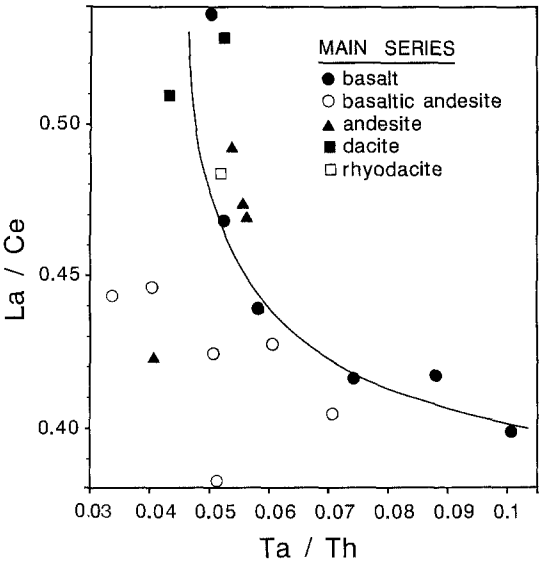

Fig. 8. La/Ce vs Ta/Th for Main Series lavas. The trend is parabolic, suggestive of processes involving mixing between more than one compositional end-member. Based on data from Mann (1983)

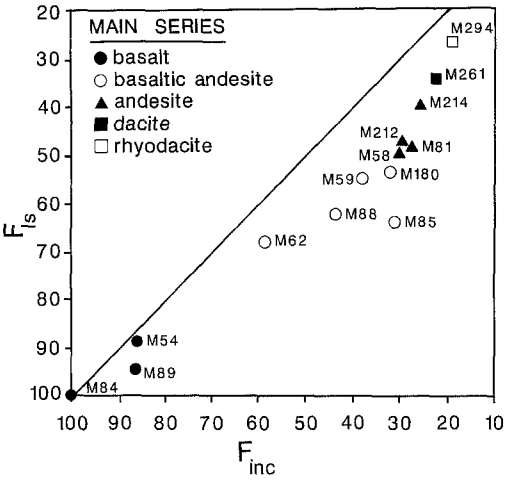

Fig. 10. Decoupling between major and trace element fractionation models of the Main Series lavas (based on compositional data in Nicholls 1971; and Mann 1983) is shown as a plot of F_{ls} (% fractionation calculated by least squares from bulk major element compositions) vs F_{inc} (calculated from Th abundances). M84 is the hypothetical parent composition

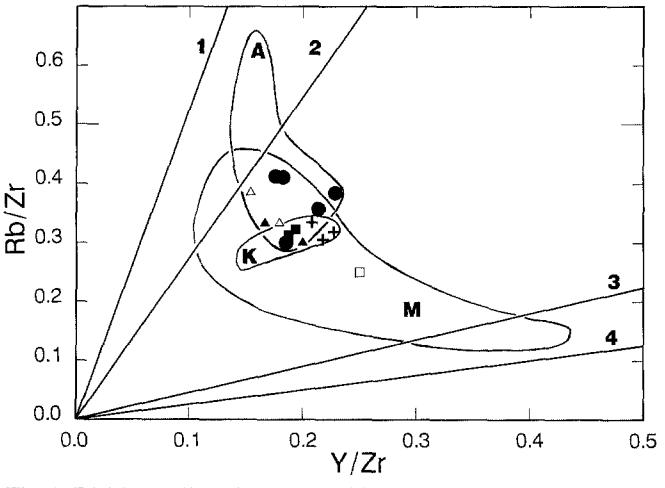

Fig. 9. Rb/Zr vs Y/Zr, depicting fields of Akrotiri (*A*), Main Series (*M*), and Kameni (*K*) lavas. The fields are based on data in Barton and Huijsmans (1986), Mann (1983), and Huijsmans et al. (1988). *Lines* labelled *1* and *2* represent Rb/Y ratios of 5.3 and 2.8, taken as average continental crust (Pearce et al. 1984) and average Canadian shield (Shaw et al. 1976; Shaw 1980). *Lines 3* and *4* represent ratios of 0.44 and 0.24, representative of Hawaiian tholeiites (Basaltic volcanism Study Project, 1981). The *symbols* refer to the samples used in the present study (see Fig. 2 for key)

Modelling of crystal fractionation by least squares mixing (Wright and Doherty 1970) for two fractionation intervals, basalt to andesite (with 58 wt% SiO_2) and andesite to dacite, employing microprobe compositional data of observed phenocryst assemblages, however, results in high residuals if fractionation is the only process invoked to account for the compositional spectrum. This is anticipated in view of the fact that these assemblages are partly xenocrystic, as will be discussed in the next section. Residuals improve if mixing with rhyodacitic liquid of composition similar to the Upper (Minoan) Pumice is invoked in addition to fractionation. Furthermore, the percentage of fractionation (F) from an observed hypothetical parent composition, as calculated by the least squares method for major elements in a suite of Main Series lava samples (compositional data from Nicholls 1971), when compared to F calculated from the variation in Th abundances of the same samples (reported in Mann 1983), reveals significant decoupling between the major and trace element fractionation model results (Fig. 10).

Mineral chemistry

The petrography of Thera volcanics has been described by Nicholls (1971) and briefly by Pichler and Kussmaul (1972). Mor recently, the petrography and mineral chemistry of the postcaldera dacites have been detailed by Barton and Huijsmans (1986). Below we summarize the mineralogy and mineral chemistry of the lava samples selected for study.

Ferromagnesian minerals

Corroded phenocrysts and microphenocrysts of olivine occur in the most basic (basalt to basaltic andesite) flows, and are rare and distinctly xenocrystic in more felsic units. Phenocrysts in sample MP-1 (basalt from Skaros) invariably exhibit resorption and corrosion features with relatively flat compositional profiles ranging from Fo_{75} to Fo_{80}, and narrow rims, steeply zoned down to Fo_{70}. Subhedral and lobate, resorbed microphenocrysts occur in the groundmass with compositions ranging from Fo_{74} to Fo_{79}, with the subhedral crystals generally being less forsteritic than resorbed ones. The olivine composition in equilibrium with a bulk composition corresponding to basalt MP-1 (Mg number = 52), calculated according to Roeder and Emslie's (1970) method, is Fo_{74}, which coincides with the composition of the subhedral microphenocrysts. The olivines displaying resorption and corrosion features may be xenocrystic. The pyroxenes in the samples examined do not display obvious zoning or resorption.

Plagioclase: general observations

Heterogeneous plagioclase populations are charateristic of the volcanic products of Thera. Compositionally, plagioclase crystal cores range from An_{28} to An_{86} and a large part of this range is represented in each of the samples studied, whether its bulk composition is basaltic, andesitic, or dacitic. Three major compositional groups may be distinguished: those with cores of An_{28-45}, those with An_{49-63}, and those with An_{69-86} (Fig. 11). Furthermore, characteristic textures are displayed by crystals in each group, de-

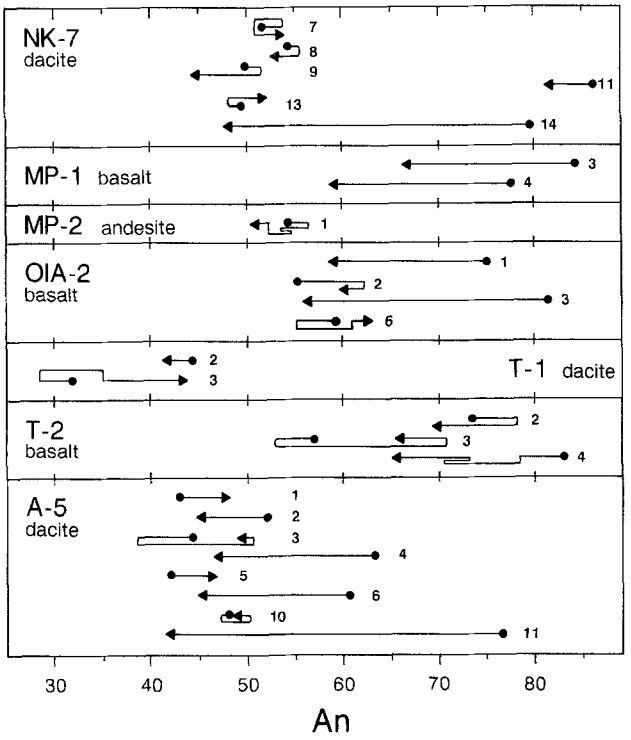

Fig. 11. Simplified compositional trends in selected plagioclase crystals from samples studied showing that heterogeneous plagioclase populations are typical. *Circles* represent cores of crystals and *arrowheads* represent rims. *Lines* join analyses of same crystal and indicate compositional trend from core to rim. *Numbers* refer to the crystal number in the thin section for comparison with Nomarski images

pending on the bulk composition of the lava in which they are hosted (i.e., basic, intermediate, or acidic).

Combined optical and Nomarski observations as well as electron microprobe data allow the distinction of different plagioclase crystal populations in both basalts and dacites. On this basis, the plagioclase crystals in lavas from Thera can be grouped into three categories:

I) inherited (nucleated prior to initial mixing event, Type Ia from the more basic end-member. Type Ib from the more felsic end-member),

II) in situ plagioclase (nucleated in mixed or hybrid magma), and

III) xenocrystic (greater than An_{85}).

Plagioclases typically display oscillatory-normal or oscillatory-even zoning (Figs. 3–7) in addition to other zoning features which will be discussed later. In general there is a similarity between zoning in mantles of large phenocrysts and complete zoning patterns of the smaller euhedral phenocrysts.

Plagioclase core compositions in basalts and basaltic andesites range from An_{50} to An_{92}. Calculated (dry) plagioclase compositions in equilibrium with the observed basaltic bulk compositions range from An_{60} to An_{70}. Observed mantles have similar or less calcic compositions and range from An_{60} to An_{70}. We interpret rounded forms, irregular rounded edges, re-entrants, and multiply intercepted re-entrants (sieve texture) as resorption (and/or reaction) features, although these might be alternatively interpreted as growth forms. Melt inclusions assume variable morphologies, from rounded to elongate. On different scales they define "sieve-textured" zones (e.g., "spongy" cores, or dusty cores or zones). A higher proportion of plagioclase phenocrysts in basalts display "sieve-textured" or "fritted" or "mottled" cores (penetrative resorption features in core, Fig. 12). Resorption surfaces (labelled R in Figs. 3–7) conformably and unconformably intersect growth zones and earlier resorption surfaces and exhibit variable morphologies, from smooth (curvilinear, cuspate or planar) to irregular (rough, sieve, jagged, crenulated, etc.). Fine "sieve-textured" interfaces between growth zones are very similar to the "rough" interfaces observed by Tsuchiyama (1985) in his plagioclase dissolution experiments, which result from mixing with magma more calcic than the equilibrium liquid. Irregular solution interfaces are more common in crystals hosted by basaltic lavas.

The types of plagioclase crystals described above are observed in the dacite samples from all of the centers studied. Type III calcic plagioclase, however, is represented by xenocrysts that originated in basaltic liquids. Plagioclase compositions calculated to be in dry equilibrium with given dacitic bulk compositions are more sodic (An_{29}) than observed compositions of plagioclase in equilibrium with interstitial liquids.

Cursory differentiation of plagioclase crystals on the basis of textural features (Fig. 13) reveals significant overall differences in plagioclase population distributions in basic and acidic lavas. Plagioclase phenocrysts in dacites typically exhibit numerous solution interfaces, particularly in their outer zones (mantles). The plagioclase cores rarely display resorption textures (e.g., Nea Kameni dacites) but when they do, these are generally smooth solution interfaces.

Plagioclase: laser and Nomarski interferometry

High resolution profiles of compositional variation across plagioclase crystals were transcribed from laser interferogram fringe patterns and calibrated with electron microprobe point analyses. In general, the compositional profiles exhibit layers (<2 to 50 μm thick, most frequently between 5 and 20 μm) that are oscillatory-even, oscillatory-normal, as well as simple-even, simple-normal or reverse zoned, and separated by compositional discontinuities which corresponds to solution interfaces, as identified from Nomarski contrast images. Frequently, resorption surfaces are not associated with significant jumps in An content. In some cases, sieve-textured zones (10 to 50 μm thick) occur near the phenocryst rims. As discussed, all the lavas examined appear to exhibit up to four generations of plagioclase crystals, each of which possess general similarities in compositional profiles.

Three general types of zoning trends are commonly distinguished, from the crystal's core outward:

1) A calcic core (>An_{68}, half width 25 to 250 μm), commonly sieve-textured, even or normally zoned, followed by a resorption surface, generally associated with an abrupt drop in An content of at least 10 mole%, and succeeded by one or more layers, over which the zoning is oscillatory to simple with an overall normal trend (Type Ia, Fig. 4 and Fig. 13a). A rare variety included in this type, observed only in the most mafic lavas, exhibits a very calcic core (e.g., An_{89}) with only one major resorption surface followed by very pronounced normal zoning (Type III, Fig. 7, Fig. 13d).

2) A sodic core (An_{28-45}, half width 10 to 50 μm) followed

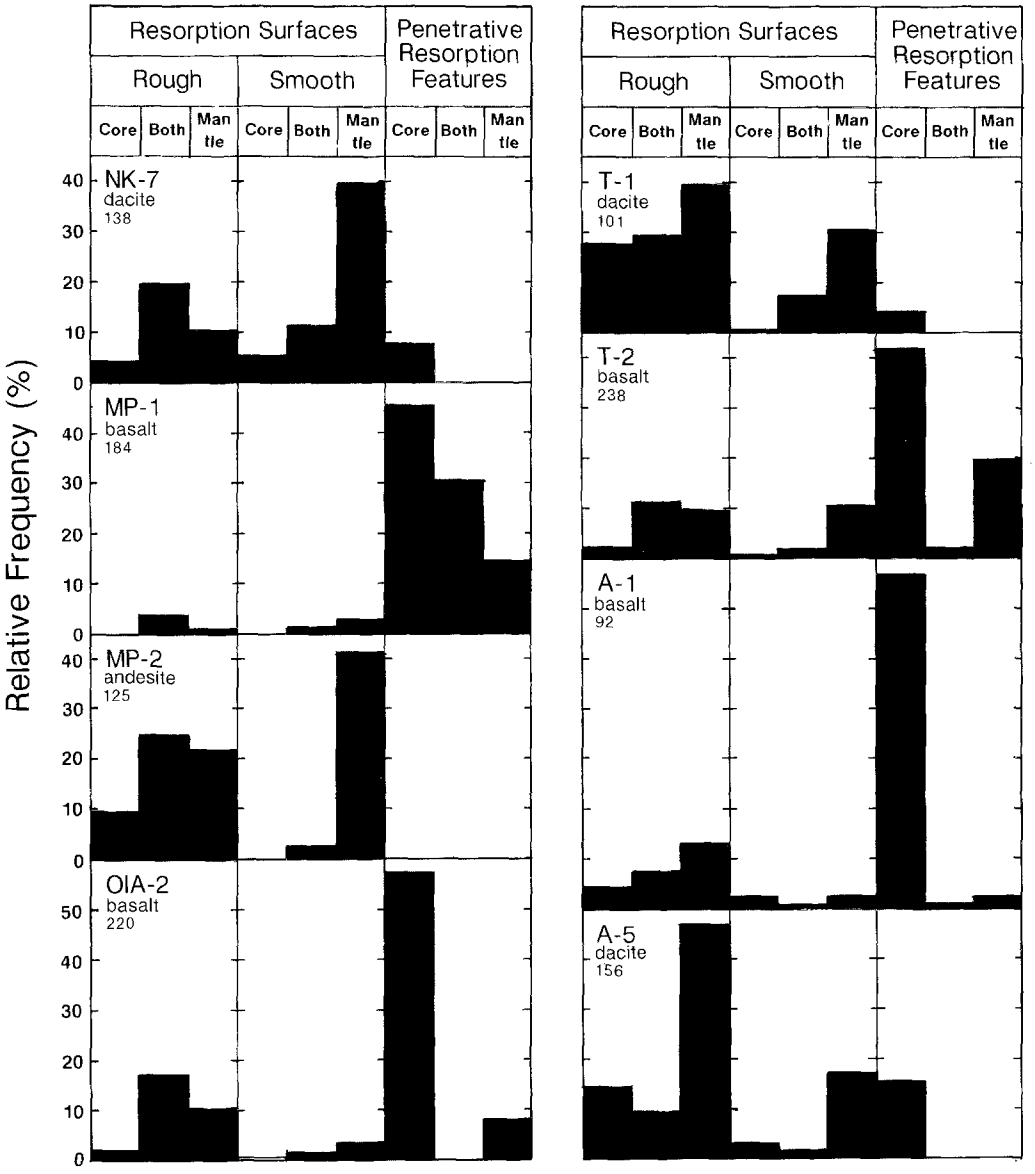

Fig. 12. Frequency distribution of plagioclase crystals with distinct textural features in Nomarski images of thin sections of eight samples. Penetrative resorption features include mottled, spongy, and fretted textures. *Numbers* beneath sample numbers refer to total number of crystals observed. Note that crystals with penetrative features in their core are more abundant in basalts than in more acidic lavas

by a complex sequence of numerous smooth to irregular resorption surfaces separating plagioclase layers with at least one abrupt increase in An content of at least 10 mole% (Type Ib, Fig. 5 and Fig. 13b).

3) An intermediate core (An_{45-65}, half width up to 50 μm), followed by a complex pattern of simple to oscillatory, normal, even, and/or reversed zones (Type II, Fig. 6 and Fig. 13c).

Interpreting zoning profiles: linearization

In interpreting mineral zoning, it has been shown that there are numerous advantages to transforming the raw data, using a numerical crystal growth model, into a material-balance constrained profile in which changes in magma composition and/or intensive variables have predictable effects. Pearce et al. (1987b) have outlined a model based on a simple normal growth law in which profiles of composition (in terms of end-members) vs distance are transformed into end-member ratio vs nominal volume crystallized. Simple normal growth requires that the end-member ratio varies as a linear function of crystallized volume in a closed system, thus simplifying some of the zonation trends. For details of the mathematical model the reader is referred to Pearce et al. (1987b). Although the quantitative interpretation of such linearized profiles is still in its early stages, there are several features from which qualitative interpretations of the pre-eruptive history of a group of crystals can be made. In a linearized plagioclase profile, for example, An/Ab (molar ratio) is plotted against nominal volume crystallized, approximated by the cube of twice the distance from the center of the crystal, in 100 μm cubes or 10^6 μm^3 (Fig. 9; also see Pearce et al. 1987b). An idealized linear profile with An/Ab decreasing as volume crystallized increases, can be interpreted as closed system crystallization from the crystal's local reservoir (i.e., the surrounding layer of melt). Extrapolation of a linear segment to its intercept on the volume axis gives an estimate of

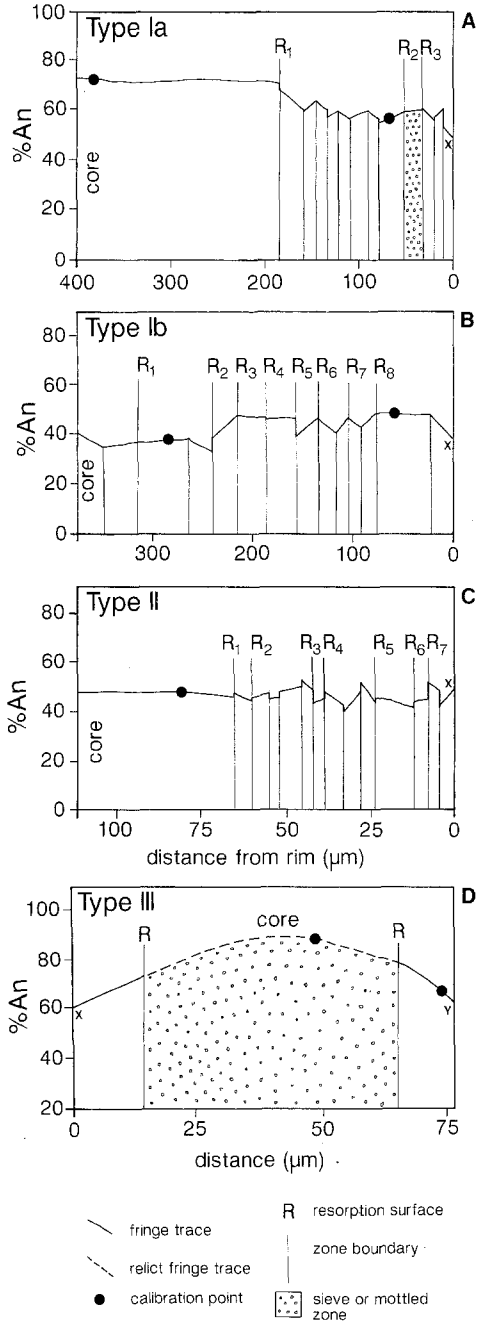

Fig. 13A–D. Digitized zoning profiles of the four crystals in Figs. 4 to 7 representative of the four populations distinguished based on combined textural and compositional zonation characteristics. **A** OIA-2-1 (in basalt). **B** A-5-3 (in dacite). **C** NK-7-13 (in dacite). **D** T-2-4 (in basalt)

the fictive volume (EFV), or the maximum amount of plagioclase that can be crystallized from a melt with the composition of the local reservoir. A discontinuity and/or change in slope of the profile therefore must reflect a transfer of mass and/or energy from the bulk magma reservoir to the crystal's local reservoir. Changes in the local reservoir are therefore directly related to changes in the bulk magmatic reservoir. Furthermore, the nature of the change in EFV after a discontinuity may be a useful indicator of the type of process involved in the transfer. For example, a first order discontinuity and subsequent increase (or decrease) in An/Ab may result from an abrupt change in the composition of the local reservoir to a more (or less) anorthitic liquid (i.e., magma mixing). A second order discontinuity (i.e., a change in slope) results in an increase or decrease in EFV without an "immediate" change in the composition of the crystallizing plagioclase. It is unlikely that this would be due to a change in composition of the liquid of the local system and so must result from a change in intensive parameters of the system. Segments of a linearized profile which are reverse zoned (i.e., have a positive slope) do not give meaningful EFVs and are clearly the product of crystallization under dynamic conditions strongly influenced by the degree of undercooling (Lofgren 1980). In the dynamic crystallization experiments of Lofgren, a decrease in undercooling resulted in reverse zoned growth. Finally, segments that are flat or with a very shallow slope, i.e., very large EFV, indicate crystallization during which the local reservoir was open or, in other words, under compositional steady-state conditions. Oscillatory zoning can be explained by kinetic crystallization effects in the immediate vicinity of the growing crystal surface, i.e., within the local reservoir (Kirkpatrick 1975; Kirkpatrick et al. 1976, 1979; Sibley et al. 1976; Haase et al. 1980; Lofgren 1980; Allégre et al. 1981; Loomis 1981, 1982; Smith and Lofgren 1983).

Discussion

Major and compatible trace element distributions in the volcanic products of Thera mainly reflect crystal fractionation processes (Nicholls 1971; Huijsmans et al. 1988) and are generally insensitive to processes involving mixing between magmas. Incompatible trace elements are more sensitive petrogenetic tracers in this respect; decoupling of trace and major element variations and parabolic distributions of incompatible trace element ratios (Figs. 8 to 10), are both suggestive of processes involving mixing of compositionally discrete magmas. This is further supported by recently published U-Th isotopic systematics of mineral separates from the Mikros Profitis Ilias lavas. The isotopic variations have been interpreted as resulting from mixing between dacitic and andesitic end-members (Pyle et al. 1988).

In addition, inhomogenous phenocryst populations (Figs. 11 and 12), crystals which were apparently out of equilibrium with their surrounding melts and exotic mineralogy such as zircon in andesites (Pyle et al. 1988), also present a strong case for magma mixing processes.

Plagioclase zoning is envisaged as the micro-dial that tunes us into these associated petrogenetic processes. Examination of the linearized profiles (Fig. 14) reveals striking overall differences between calcic and sodic plagioclases:

(a) In mafic lavas, plagioclases with calcic cores (Type Ia, Fig. 14a) generally possess a smaller number of resorption surfaces than those with more sodic cores. Paucity of resorption surfaces in plagioclase phenocrysts in mafic lavas may be due to relatively shorter residence times of these magmas in the subvolcanic reservoir or, alternatively, may reflect the lower volatile solubilities in mafic magmas. The smaller amounts of H_2O available for release during degassing of mafic magma could result in less pronounced effects on the liquidus plagioclase composition than in water-rich felsic magmas.

(b) Plagioclases with spongy, fritted, or mottled cores (Types Ia & III) are significantly more abundant in basic lavas. Such pervasive resorption features can be caused by melting of crystals due to temperature increase (Maaloe

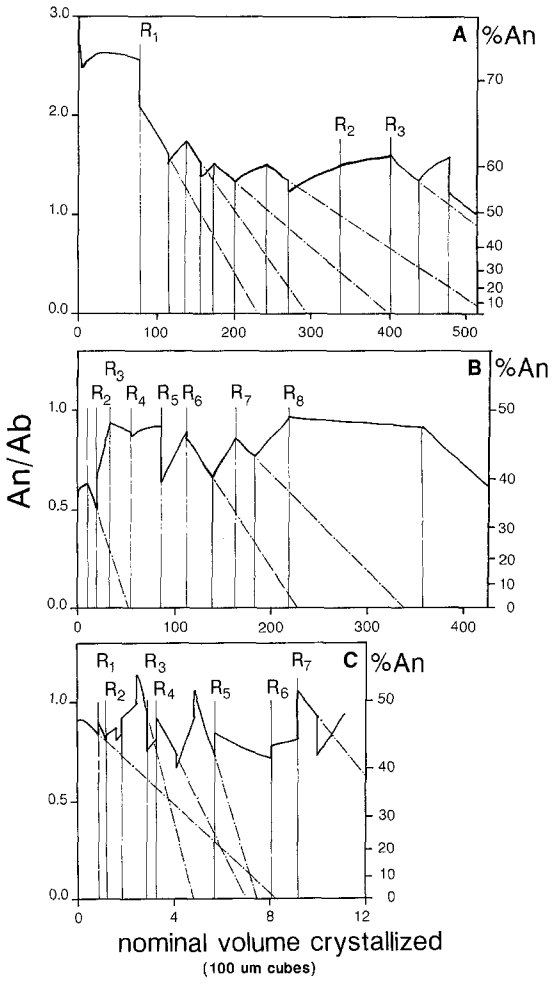

Fig. 14A–C. Linearized transformations of the digitized profiles in Fig. 13A–C. **A** Plagioclase OIA-2-1, representative of Type Ia. **B** Plagioclase A-5-3, representative of Type Ib. **C** Plagioclase NK-7-13, representative of Type II. Symbols same as in Fig. 13; *dot-dashed line* extrapolation of portions of the profiles approximating simple normal growth to their EFVs. See text for further discussion

1976; Lofgren and Norris 1981; Tsuchiyama 1985) or, as interpreted by some workers, decompression (Vance 1965; Pearce et al.1987a) despite the relatively small effect of pressure on the basalt liquidus (2 to 7 degrees per kilobar, Thompson and Kushiro 1972). Osborn (1976), on the basis of phase equilibria suggested that the parental magmas for the Thera Series began crystallizing under at least 8 kbars pressure, corresponding to the depth of the crust-mantle interface beneath Thera (~26 km, Mercier et al. 1987). In Thera lavas, therefore, the presence of very calcic plagioclases (up to $\sim An_{90}$) with resorbed cores, as well as plagioclases with intact cores but with cloudy, melt inclusion rich mantles, can be explained by either decompression or temperature increase. At any rate, the association of pervasive resorption features with intratelluric plagioclase crystallized from basic liquids may be used empirically to estimate the relative proportion of plagioclase phenocrysts in a particular mixed lava that were inherited from the basic end-member.

(c) Plagioclases from felsic lavas characteristically display pairs of alternating normal and reverse zoned growth layers, separated by resorption surfaces in their mantles (Fig. 14b, c). These are consistent with normal crystallization (normal zoning) with an accompanying buildup of dissolved volatiles (H_2O), causing a decrease in undercooling and disequilibrium crystallization, which results in reverse zoned growth (Loomis 1982); as volatile saturation is reached, degassing (and possibly eruption) may result in the formation of a resorption surface. In the same profiles, first order discontinuities (ΔAn on the order of 10 mole % or more) associated with resorption surfaces and followed by a reverse zoned growth layer probably record magma mixing events with hotter, mafic magma and subsequent increase in temperature (i.e., decrease in the undercooling and precipitation of more anorthitic plagioclase). Portions of zoning profiles that are rather flat probably represent crystallization in a steady state system (Fig. 14b).

(d) The magnitude of the compositional discontinuities in An content across mixing-related resorption surfaces are rather modest in the Thera plagioclases (ΔAn up to ~10 mole %) in comparison to those reported for similar phenomena in hybrid andesites and dacites (Nixon & Pearce 1987). This is because plagioclases hosted in basalts and dacites of Thera crystallized from melts which were near the end-member compositions and did not suffer extensive subsequent hybridization (e.g., to andesite).

(e) Resorption surfaces such as R_1 to R_6 in the plagioclase crystal from Nea Kameni dacite (Fig. 12c) most likely record influxes of mafic magma without complete mixing, i.e, predominantly thermal perturbations experienced by dacitic magma.

A large, felsic, stratified magma chamber such as the one presently beneath Thera (Yokoyama and Bonasia 1978) will act as a density barrier to the mafic magma periodically injected into its depths (Wiebe 1987). Influxes of hot, mafic magma, however, would cause thermal perturbations which would initiate thermal convection and automixing within the overlying silicic magma and could eventually result in eruption by thermally induced explosive degassing. Calcic plagioclase xenocrysts in the Kameni dacites were, therefore, inherited from an earlier mixing event, possibly during the re-establishment of the crustal reservoir shortly after the Minoan caldera-forming eruption (Bo caldera, Fig. 2).

We have used compositional zoning in plagioclase as a record of magmatic processes, magma mixing in particular, in the subvolcanic reservoir beneath the volcano of Thera. The presence of a second magma reservoir at deeper levels is implicit in the discussion of our data. Phase equilibria studies in the system $MgO-FeO-Fe_2O_3-CaAl_2Si_2O_8-SiO_2$, at total pressures of 1 bar and 10 kbars and $f(O_2)=0.21$ bars (Osborn 1976) suggest that the parental magmas for the Thera Series began crystallizing at 8 kbars or more which constrains the depth of this deeper reservoir to the crust-mantle interface beneath Thera (~26 km, Mercier et al. 1987). Such large subcrustal reservoirs are envisioned as pools of mantle-originated basaltic melts arrested by the crustal density filter and causing its partial melting, indirectly producing felsic magmas (Arth and Hanson 1972; Oskarsson et al. 1979; St. Seymour and Francis 1988).

Variations in incompatible trace element abundance ratios of lavas from Thera suggest the involvement of two compositionally contrasting sources in their genesis (Figs. 8 and 9). Crustal control is more pronounced in the felsic magmas produced early on the history of the volcanic complex of Thera (Akrotiri lavas) and is probably an expression both of the fertility of the crustal source and the immaturity of magma conduits through the crust. As the magmatic

plumbing system matured, and the crustal source presumably became progressively more depleted through repetitive melting, crustal control became less apparent (Kameni dacites, Fig. 9). Maturation of subvolcanic reservoirs through enlargment and development of compositional stratification reduces the capacity for thorough mixing with fresh batches of mafic magma and is a possible explanation of the smaller proportion of plagioclase crystals displaying "rough" solution interfaces (Tsuchiyama 1985) in the Nea Kameni dacite (NK-7) than in the Akrotiri dacite (A-5) (Fig. 12).

Major and trace element systematics of lavas from the volcanic complex of Thera indicate that mixing of magmas of contrasting compositions in addition to crystal fractionation were both operative in their genesis. Involvement of magma mixing is corroborated by evidence based on phenocryst sub-populations in chemical and textural disequilibrium with their host lavas. Our work has shown that, regardless of bulk composition and stratigraphic position, crystals representative of each of the sub-populations may be found in all lavas, i.e., the textural features are largely the result of recurrent processes such as flushing of the system with new magma, and cannot generally be attributed to specific events. Plagioclase zoning profiles record the attempts of a compositionally complex liquidus mineral to equilibrate with a host magma whose physical and compositional parameters were changing periodically. At Thera, the plagioclase zoning profiles record only modest jumps in An, indicating that hybridization is not extensive and that most of the mixed lavas are near an end-member composition. Plagioclases from basic lavas show more evidence of decompression and/or thorough mixing with drafts of more primitive magma, possibly shorter residence times in the subvolcanic reservoir, and smaller effects of volatiles on liquidus plagioclase compositions. These features are all consistent with an initially open magma chamber which was largely degassed and actively convecting. Plagioclase in felsic lavas record influxes of hotter mafic magma, but not necessarily thorough mixing, and periodic volatile accumulation and release, consistent with a more static, compositionally zoned, i.e., mature, subvolcanic magma chamber.

Acknowledgements. The first author (KStS) thanks the Greek Geological Survey (IGME) for permission to work on the island of Thera. KStS and THP acknowledge the support of the Natural Sciences and Engineering Research Council in the form of operating grants (KStS and THP) and equipment and infrastructure grants (THP). KStS also acknowledges support from Concordia University internal grants. Thanks to Grant Heiken and Don Francis for reviewing an earlier version of the manuscript, Bob Martin for his encouragement and two anonymous reviewers for helpful comments. Theodore Kefalas, Lori Bertrand, George Panagiotidis, M. Carter, V. Mlakar, I. Wolfson, and C. Luce are acknowledged for technical assistance in data acquisition and manuscript preparation. The unwavering support of Charles Betrand and Elaine Newman of Concordia University enabled KStS to complete this manuscript.

References

Allègre CJ, Provost A, Jaupart C (1981) Oscillatory zoning: a pathological case of crystal growth. Nature 294:223–228

Anderson AT Jr (1983) Oscillatory zoning of plagioclase: Nomarski interference contrast microscopy of etched polished sections. Am Mineral 68:125–129

Arth JT, Hanson GN (1972) Quartz diorites derived by partial melting of eclogite or amphibolite of mantle depths. Contrib Mineral Petrol 37:161–174

Barton M, Huijsmans JPP (1986) Post-caldera dacites from the Santorini volcanic complex, Aegean Sea, Greece: an example of the eruption of lavas of near-constant composition over a 2200 year period. Contrib Mineral Petrol 94:472–495

Basaltic Volcanism Study Project (1981) Basaltic volcanism on the terrestrial planets. Pergamon, New York, 1286 pp

Clark AH, Pearce TH, Roeder PL, Wolfson I (1986) Oscillatory zoning and other microstructures in magmatic olivine and augite: Normarski interference contrast observations on etched polished surfaces. Am Mineral 7:734–741

Gill JB (1981) Orogenic andesites and plate tectonics. (Minerals and rocks, vol 16). Springer, Berlin Heidelberg New York, 390 pp

Haase CS, Chadam J, Feinn D, Ortoleva P (1980) Oscillatory zoning in plagioclase feldspar. Science 209:272–274

Hammer CU, Clausen HB, Frierich WL, Tauber H (1987) The Minoan eruption of Santorini in Greece dated to 1645 BC? Nature 328:517–517

Heiken G, Mc Coy F Jr (1984) Caldera development during the Minoan eruption, Thira, Cyclades, Greece. J Geophys Res 89:8441–8462

Huijsmans JPP, Barton M, Salters VJM (1988) Geochemistry and evolution of the calc-alkaline volcanic complex of Santorini, Aegean Sea, Greece. J Volcanol Geotherm Res 34:283–306

Kirkpatrick RJ (1975) Crystal growth from the melt: a review. Am Mineral 60:798–814

Kirkpatrick RJ, Robinson GR, Hays JF (1976) Kinetics of crystal growth from silicate melts: anorthite and diopside. J Geophys Res 84:3671–3676

Kirkpatrick RJ, Klein L, Uhlmann DR, Hays JF (1979) Rates and processes of crystal growth in the system anorthite-albite. J Geophys Res 84:3671–3676

Langmuir CH, Vocke RD, Hanson GN, Hart SR (1977) A general mixing equation: applied to the petrogenesis of basalts from Iceland and Reykjanes Ridge. Earth Plan Sci Lett 37:380–392

Loomis TP (1981) An investigation of disequilibrium growth processes of plagioclase in the system Anorthite-Albite-Water by methods of numerical simulation. Contrib Mineral Petrol 76:196–205

Loomis TP (1982) Numerical simulations of crystallization processes of plagioclase in complex melts: the origin of major and oscillatory zoning in plagioclase. Contrib Mineral Petrol 81:219–229

Lofgren GE (1980) Experimental studies on the dynamic crystallization of silicate melts. In: Hargraves RB (ed) Physics of magmatic processes. Princeton, University Press, New Jersey, pp 487–551

Lofgren GE, Norris PN (1981) Experimental duplication of plagioclase sieve and overgrowth textures. Geol Soc Am Abs Progr 13:498

Maaloe S (1976) The zoned plagioclase of the Skaergaard intrusion, East Greenland. J Petrol 17:398–419

MacDonald GA and Katsura T (1965) Eruption of Lassen Peak, Cascade Range, California in 1915: example of mixed magmas. GSA Bull 76:475–482

Mann AC (1983) Trace element geochemistry of high alumina basalt-andesite-dacite-rhyodacite of the Main Volcanic Series of Santorini volcano, Greece. Contrib Mineral Petrol 84:43–57

Mercier JL, Sorel D and Simeakis K (1987) Changes in the state of stress in the overriding plate of a subduction zone: the Aegean Arc from the Pliocene to present. Ann Tectonicae 1:20–39

Nicholls IA (1971) Petrology of Santorini volcano, Cyclades, Greece. J Petrol 12:67–119

Nixon G, Pearce TH (1987) Laser-interferometry of oscillatory zoning in plagioclase: the record of magma mixing and phenocryst recycling in calc-alkaline magma chambers, Iztaccihuatl volcano Mexico. Am Mineral 72:1144–1162

Osborn EF (1976) Origin of calc-alkali magma series of Santorini volcano in the light of recent experimental phase-equilibrium studies. In: Proc Int Congr Therm Waters, Geotherm Energy, Volcanism Med Area, vol 3, Athens, pp 154–167

Oskarsson N, Sigvaldason GE, Steinthorsson S (1979) A dynamic model of rift zone petrogenesis and the regional petrology of Iceland. Nordic Volcanological Institute 7905 and Science Institute 7916, University of Iceland

Pearce TH (1984) Optical dispersion and zoning in magmatic plagioclase: laser interference observations. Can Mineral 22:383–390

Pearce JA, Harris NBW, Tindle AG (1984) Trace element discrimination diagrams for the tectonic interpretation of granitic rocks. J Petrol 25:956–983

Pearce TH, Russell JK, Wolfson I (1987a) Laser interference and Nomarski interference imaging of zoning profiles in plagioclase phenocrysts from the May 18, 1980, eruption of Mount St Helens, Washington. Am Mineral 72:1131–1143

Pearce TH, Griffin MP, Kolisnik AM (1987b) Magmatic crystal stratigraphy and constraints on magma chamber dynamics. Laser interference results on individual phenocrysts. J Geophys Res 92:745–758

Pichler H, Kussmaul S (1972) The calcalkaline volcanic rocks of the Santorini group (Aegean Sea, Greece). Neues Jahrb Mineral Abh 116:268–307

Pyle DM, Ivanovich M, Spark RSJ (1988) Magma-cumulate mixing identified by U-Th disequilibrium dating. Nature 331:157–159

Roeder PL, Emslie RF (1970) Olivine-liquid equilibrium. Contrib Mineral Petrol 29:275–289

Seward D, Wagner G, Pichler H (1980) Fission-track ages of Santorini volcanics (Greece). In: Doumas C (ed) Thera and the Aegean world 2. Aris & Phillips, London, pp 101–108

Shaw DM (1980) Development of early continental crust III. Depletion of incompatible elements in the mantle. Precambrian Res 10:281–299

Shaw DM, Dostal J, Keays RR (1976) Additional estimates of continental surface Precambrian shield composition in Canada. Geochim Cosmochim Acta 40:78–83

Sibley DF, Vogel TA, Walker BM, Byerly G (1976) The origin of oscillatory zoning in plagioclase: a diffusion and growth controlled model. Am J Sci 276:275–284

Smith RK, Lofgren GE (1983) An analytical and experimental study of zoning in plagioclase. Lithos 16:153–168

Stamatelopoulou Seymour K, Francis D (1988) Magmatic interaction between mantle and crust during the evolution of the Archean Lac Guyer greenstone belt, New Quebec. Can J Earth Sci 25:691–700

Thompson RN, Kushiro I (1972) Origin of some abyssal tholeiites from the Mid-Atlantic ridge. Yearb Carnegie Inst Washington 71:403–406

Tsuchiyama A (1985) Dissolution kinetics of plagioclase in the melt of the system Diopside-Albite-Anorthite, and origin of dusty plagioclase in andesites. Contrib Mineral Petrol 89:1–16

Vance JA (1965) Zoning in igneous plagioclase: patchy zoning. J Geol 73:637–651

Watkins ND, Sparks RSJ, Sigurdsson H, Huang TC, Federman A, Carey S and Ninkovich D (1981) Volume and extent of the Minoan tephra from Santorini volcano: new evidence from deep-sea sediment cores. Nature 271:122–126

Wiebe RA (1987) Rupture and inflation of a basic magma chamber by silicic liquid. Nature 326:69–71

Wright TL, Doherty PC (1970) A linear programming and least squares computer method for solving petrological mixing problems. Geol Soc Am Bull 81:1995–2008

Yokoyama I, Bonasia V (1978) Gravity anomalies of the Thera islands. In: Doumas C (ed) Thera and the Aegean world 1. Aris & Phillips, London, pp 147–150

Received January 3, 1989 / Accepted June 28, 1989
Editorial responsibility: I.S.E. Carmichael